Available online at www.sciencedirect.com
SCIENCE DIRECT
Physics Letters B 636 (2006) 293–298
PHYSICS LETTERS B
www.elsevier.com/locate/physletb

Non-adiabatic dynamics in ^{10}Be with the microscopic $\alpha + \alpha + N + N$ model

Makoto Ito [1]

Institute of Physics, University of Tsukuba, 305-8571 Tsukuba, Japan

Received 18 August 2005; received in revised form 2 February 2006; accepted 29 March 2006

Available online 7 April 2006

Editor: J.-P. Blaizot

Abstract

The $\alpha + {}^6$He low-energy reactions and the structural changes of ^{10}Be in the microscopic $\alpha + \alpha + N + N$ model are studied by the generalized two-center cluster model with the Kohn–Hulthén–Kato variation method. It is found that, in the inelastic scattering to the $\alpha + {}^6\mathrm{He}(2_1^+)$ channel, characteristic enhancements are expected as the results of the parity-dependent non-adiabatic dynamics. In the positive parity state, the enhancement originates from the excited eigenstate generated by the radial excitation of the relative motion between two α-cores. On the other hand, the enhancement in the negative parity state is induced by the Landau–Zener level-crossing. These non-adiabatic processes are discussed in connection to the formation of the inversion doublet in the compound system of ^{10}Be.

PACS: 21.60.Gx; 24.10.Eq; 25.60.Je

In the last two decades, developments of experiments with secondary RI beam have extensively proceeded the studies on light neutron-rich nuclei. In particular, much efforts have been devoted to the investigation of molecular structure in Be isotopes. Theoretically, molecular models with π and σ orbitals along the axis connecting two α-particles have been successful in understanding the low-lying states of this isotopes [1,2]. Experimentally, the molecular structures were mainly investigated by the breakup processes [3,4] and the sequential decays [5] using the high energy RI beams.

In recent experiments, furthermore, the low-energy ^{6}He beam becomes available. Low-energy reaction cross-sections such as the elastic scattering with an α target [6,7] and the sub-barrier fusions with heavy target [8] have been accumulated. In future experiments, it will also be possible to investigate the molecular states in Be isotopes through the reactions such as $\alpha + {}^6$He [9] and $\alpha + {}^8$He [10] with low-energy ^{6,8}He-beams. Therefore, it is very interesting to study theoretically on the low-energy scattering of ^{6}He and ^{8}He by an α target.

In studying reaction processes exciting the molecular degrees of freedom, it is very important to construct a unified model which is capable of describing both structure and reaction on the same footing. For this purpose, we introduce a microscopic model, the generalized two-center cluster model (GTCM) [11,12]. In this model, it is possible to describe both molecular and atomic limit of the system of $C_1 + C_2 + N + N + \cdots$ where C_i is the ith cluster core and N is the nucleon. In the region where two core nuclei are close, the total system is expected to form the molecular orbital structure, while in the region where two core nuclei are far apart, the molecular orbitals smoothly change into product wave functions consisting of the atomic orbitals.

In this Letter, we apply the GTCM for the ^{10}Be nucleus with the $\alpha + \alpha + N + N$ four-body model. We will analyze both molecular structure in ^{10}Be and the low-energy $\alpha + {}^6$He scattering. Besides the description of the $\alpha + {}^6$He reaction, such analysis will be useful to understand the breakup mechanism of ^{10}Be into clusters. In spite of many theoretical efforts in the last decade [1,2,13–16], only Ref. [13] discusses the molecular-orbital formation in ^{10}Be and the $\alpha + {}^6$He scattering problem in a unified way.

Current experimental investigations are extended to the ^{12}Be and ^{14}Be nuclei [4,6] and hence, theoretical studies extended to such heavier systems are urged. The GTCM approach has a potential to ^{12}Be and ^{14}Be as well as ^{10}Be. On the other hand, the

E-mail address: itom@nucl.ph.tsukuba.ac.jp (M. Ito).

[1] Present address: RIKEN, Hirosawa 2-1, Wako, Saitama 351-0198, Japan.

0370-2693
doi:10.1016/j.physletb.2006.03.063

direct extension of the approach in Ref. [13] becomes quite difficult for systems with many valence neutrons, since it utilizes the $\alpha + \alpha + N + N$ few-body model.

One of the favorable features of our approach is that it is possible to describe the nuclear Landau–Zener (LZ) transition microscopically [17–22]. The LZ transition is induced by the avoided level-crossing of two adiabatic potential-surfaces. When the avoided crossing occurs in the potential surfaces, the adiabatic states drastically change their intrinsic character at the crossing point. For large relative velocity, the colliding nuclei follows not the adiabatic path but the diabatic one. This diabatic motion was discussed by Landau and Zener for the atomic collision [23]. The nuclear analogue has been called the nuclear LZ transition. In spite of long history on this issue, a clear evidence of the LZ transition is still lacking in nuclear collision [24,25]. Our microscopic approach will indicate a possible nuclear LZ transition in the collision of $\alpha + {}^6$He.

First, we briefly explain the framework of GTCM [11,12]. The basis functions for ^{10}Be are given as

$$\Phi^{J^\pi K}_{m,n}(S) = \hat{P}^{J^\pi}_K \cdot \mathcal{A}\{\psi_L(\alpha)\psi_R(\alpha)\varphi(m)\varphi(n)\}. \quad (1)$$

The α-cluster wave function $\psi_i(\alpha)$ $(i = L, R)$ is given by the $(0s)^4$ configuration in the harmonic oscillator (HO) potential. The position of an α-cluster is explicitly specified as the left (L) or right (R) side. The relative motion between α particles is described by a localized Gaussian function specified by the distance S [26]. A single-particle state for valence neutrons around one of α clusters is given by an atomic orbitals (AO), $\varphi(i, p_k, \tau)$ with the subscripts of a center i $(= L$ or $R)$, a direction p_k $(k = x, y, z)$ of 0p-orbitals and a neutron spin τ $(= \uparrow$ or $\downarrow)$. In Eq. (1), the index $m(n)$ is an abbreviation of the AO (i, p_k, τ). The intrinsic basis functions with the full antisymmetrization $\mathcal{A}$ are projected to the eigenstate of the total spin J, its intrinsic angular projection K and the total parity π by the projection operator $\hat{P}^{J^\pi}_K$.

The total wave function is finally given by taking a superposition over S and K as

$$\Psi^{J^\pi} = \int dS \sum_{iK} C^K_i(S)\Phi^{J^\pi K}_i(S) \quad (2)$$

with $i \equiv (m, n)$. The coefficients $C^K_i(S)$ are determined by solving a coupled channel GCM (generator coordinate method) equation [26]. If we fix the generator coordinate S and diagonalize the Hamiltonian with respect to i and K, we obtain the energy eigenvalues as a function of S, which we call the adiabatic energy surfaces (AES).

In the present calculation, we used the Volkov No. 2 and the G3RS for the central and the spin–orbit part of the nucleon–nucleon (NN) interaction, respectively. The parameters in the NN interactions are modified from those in Ref. [11] so as to reproduce the threshold of $\alpha + {}^6\mathrm{He}_{\mathrm{g.s.}}$ and the excitation energy of the ${}^6\mathrm{He}(2^+_1)$ state [12]. This is because the reproduction of the threshold is essentially important in the treatment of the scattering problem.

The Majorana (M), Bartlett (B) and Heisenberg (H) exchanges in the central part are fixed to $M = 0.643$, $B = -H =$ 0.125, while the strength of the spin–orbit force is chosen to 3000 MeV for the repulsive part and 2000 MeV for the attractive part. The radius parameter b of HO wave functions for α clusters and valence neutrons is commonly taken as 1.46 fm. We included all the AO configurations of two neutrons that can be constructed by the 0p-orbitals.

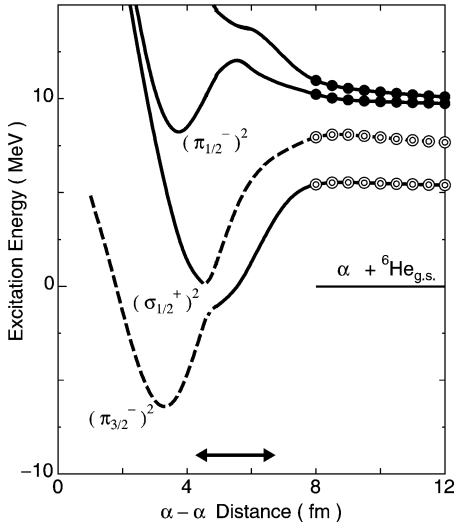

Fig. 1. Adiabatic energy surfaces for $J^\pi = 0^+$. The lowest and third local minima have a dominant configurations of $(\pi^-_{3/2})^2$ and $(\pi^-_{1/2})^2$, respectively, while the second one has a configuration of the distorted $(\sigma^+_{1/2})^2$ configuration (see text for details). The lowest and the second surfaces with the double circles are the dinuclear states of $[\alpha + {}^6\mathrm{He}(0^+_1)]_{L=0}$ and $[\alpha + {}^6\mathrm{He}(2^+_1)]_{L=2}$, respectively, while those with the solid circles have the configurations of $[{}^5\mathrm{He}(3/2^-) + {}^5\mathrm{He}(3/2^-)]$ with $(IL) = (00)$ and (22), respectively.

The AES with $J^\pi = 0^+$ is shown in Fig. 1. There appear three local minima at the short distance region of the AES. The adiabatic states (AS) at the lowest and third minima have the molecular orbital configurations of $(\pi^-_{3/2})^2$ and $(\pi^-_{1/2})^2$, respectively [1,11,12]. The AS around the second minimum has a dominant configuration of $(\sigma^+_{1/2})^2$ [1,16], but the one particle excited configuration, $(\sigma^+_{1/2}\pi^+_{1/2})$, is also strongly mixed. The latter configuration has a spin triplet structure and hence, the coupling between them is induced by the two-body spin–orbit interaction.

It is well known that the simple $\sigma^+_{1/2}$ orbital is not sufficient to describe both the 0^+_2 state in ^{10}Be and the $1/2^+$ state in ^{9}Be as discussed in Ref. [1]. Itagaki et al. shows that spin–orbit interaction generates the strong coupling between the distorted $(\sigma^+_{1/2})^2$ configuration with the spin-triplet configuration and the pure $(\sigma^+_{1/2})^2$ one, which plays very important role for lowering the 0^+_2 state in ^{10}Be [1]. Therefore, the present result is consistent to that discussed in Ref. [1] and it is reasonable to describe the intrinsic structure of $^{10}\mathrm{Be}(0^+_2)$.

At the asymptotic region ($S \geqslant 8$ fm) where two α-cores are completely separated, the valence neutrons are localized around one of the α cores. The localization of the orbitals leads to the formation of the dinuclear channels such as $[{}^4\mathrm{He} + {}^6\mathrm{He}(I)]_L$ (double circles) and $[{}^5\mathrm{He}(I_1) + {}^5\mathrm{He}(I_2)]_{IL}$ (solid circles), in which individual channels are specified by the intrinsic spin

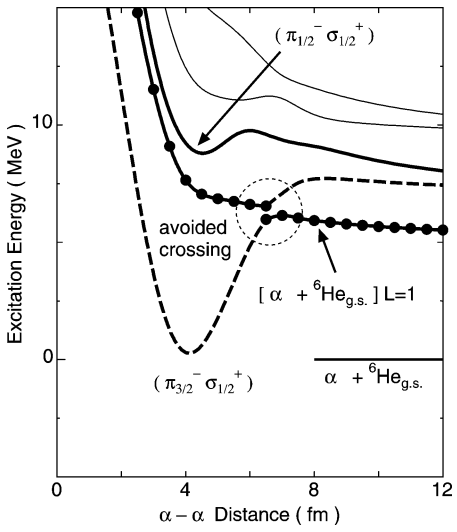

Fig. 2. The same as Fig. 1 but for the negative parity states ($J^\pi = 1^-$). The dashed (thick-solid) surfaces has a dominant component of $(\pi^-_{3/2}\sigma^+_{1/2})_{K=1}$ ($(\pi^-_{1/2}\sigma^+_{1/2})_{K=1}$) around the local minimum, while it is smoothly connected to the dinuclear channel of $[\alpha + {}^5\mathrm{He}(2^+_1)]$ with $L = 1$ ($L = 3$) at an asymptotic region. The surface with a solid circles has a dominant component of the $[\alpha + {}^6\mathrm{He}(0^+_1)]_{L=1}$ channel.

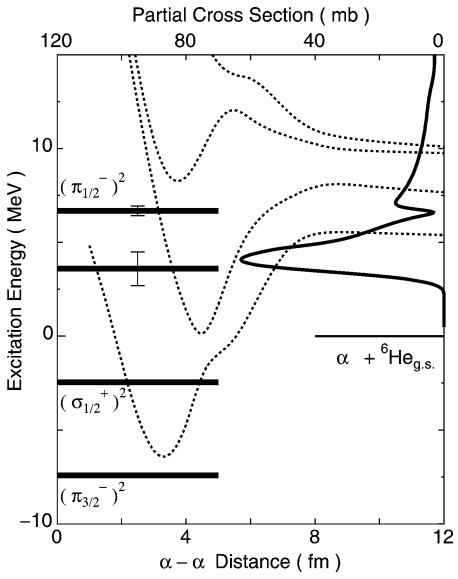

Fig. 3. Energy spectra for $J^\pi = 0^+$. The error bar means the decay width of the resonance states. The solid curve shown in the right part is the partial cross section for the inelastic scattering $[\alpha + {}^6\mathrm{He}_{\mathrm{g.s.}}]_{L=0} \to [\alpha + {}^6\mathrm{He}(2^+_1)]_{L=2}$ with a respective scale at the up-most axis. The AES in Fig. 1 are shown by the dashed curves.

of the clusters ($\mathbf{I_1}$, $\mathbf{I_2}$), the channel spin I ($\mathbf{I} = \mathbf{I_1} + \mathbf{I_2}$) and the relative angular momentum between clusters, L. The asymptotic energy position of the lowest AES is higher by about 5 MeV than the $\alpha + {}^6\mathrm{He}_{\mathrm{g.s.}}$ threshold. This is because the relative motion between clusters in Eq. (1) is described by the locally peaked Gaussian [26] and hence, its kinetic energy contributes to the AES in the asymptotic region.

The structural changes occur smoothly between the molecular orbital region and the dinuclear channels region in passing through the intermediate region shown by the arrow in Fig. 1 [11,12]. In the intermediate coupling region, we can see the level crossing between the surface of $(\pi^-_{3/2})^2$ (dashed curve) and the second one $(\sigma^+_{1/2})^2$ (solid curve). The energy splitting at the crossing point is about 1.5 MeV.

In Fig. 2, the AES for the $J^\pi = 1^-$ state is shown. The configurations of the valence neutrons smoothly changes in the AES for the α–α distance parameter except for the curves with the solid circles. The AS along this surface has an almost pure-component of the $[\alpha + {}^6\mathrm{He}(0^+_1)]_{L=1}$ channel. Thus, this AES is not molecular orbitals but the dinuclear state in the whole regions of α–α distance. Because of the different character of the lowest two orbitals, the AES behaves different as a function of α–α distance. In contrast to the results of the $J^\pi = 0^+$ states shown in Fig. 1, this causes an clear avoided-crossing at $S = 6$ fm as shown by the dotted circles in Fig. 2. The energy splitting at the crossing point is about 0.5 MeV which is smaller than that in $J^\pi = 0^+$ (∼1.5 MeV). This means that, in the negative parity state, the change of the intrinsic structure is much sharper in the distance than the case of the positive parity state.

To take into account the excitation of the relative motions between two α-cores, we solve the GCM equation by employing the AS from $S = 1$ fm to $S = 70$ fm with the mesh of 0.5 fm. The calculated energy spectra of $J^\pi = 0^+$ and $J^\pi = 1^-$ are shown in Figs. 3 and 4, respectively. In solving GCM, we apply the absorbing-kernels in the generator coordinate method (AGCM) in which the absorbing boundary condition is imposed outer region of the total system [27]. Due to the absorbing boundary, the resonance poles can be clearly identified in the complex energy plane.

In the positive parity, the 0^+_1, 0^+_2 and 0^+_4 states are the poles corresponding to the respective local minima in the AES, having the molecular orbital structures. Therefore, we should call these states the "adiabatic poles", because they can be realized as the local minima in the AES. On the other hand, there is no local minimum corresponding to the 0^+_3 state and it is generated by the radial excitation on the distance parameter S. Thus, the 0^+_3 state should be called as the "radially-excited poles", although it is the pole generated by a linear combination of the AS. The structure of 0^+_3 is very different from other lower adiabatic poles, because it is orthogonalized to the adiabatic poles and is spatially extended. The wave function in 0^+_3 has an enhanced component of $[\alpha + {}^6\mathrm{He}(2^+_1)]_{L=2}$ at the surface region and hence, it is different from the molecular orbital configuration.

In $J^\pi = 1^-$, we have identified two adiabatic poles corresponding to the two local minima of $(\pi^-_{j_z}\sigma^+_{1/2})_{K=1}$. The lower pole ($j_z = 3/2$) is generated from the linear combination of the AS around the lowest local minimum, while the higher one ($j_z = 1/2$) is originated from the minimum in the third AES as indicated by the arrow in Fig. 4.

In the present calculation, we identify no resonance corresponding to the $\alpha + {}^6\mathrm{He}_{\mathrm{g.s.}}$ AES, although its appearance is discussed within the bound state approximation in Ref. [11]. Therefore, the $\alpha + {}^6\mathrm{He}_{\mathrm{g.s.}}$ cluster configuration will not be stabilized as a resonance pole under the present condition reproducing the respective threshold energy. Since the $\alpha + {}^6\mathrm{He}_{\mathrm{g.s.}}$

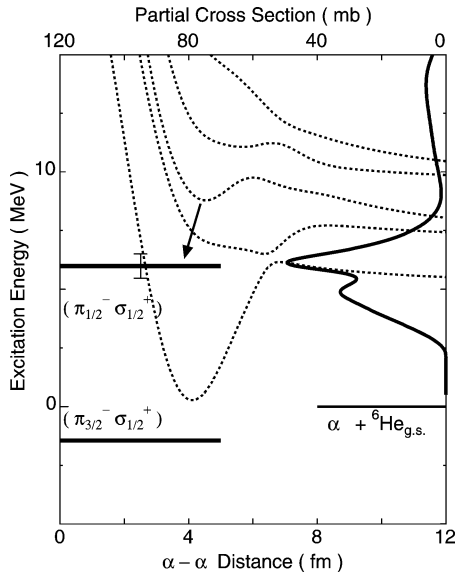

Fig. 4. The same as Fig. 3 but for $J^\pi = 1^-$. In the right part, the partial cross section for the inelastic scattering of $[\alpha + {}^6\mathrm{He}_{g.s.}]_{L=0} \to [\alpha + {}^6\mathrm{He}(2_1^+)]_{L=1}$ is shown by the solid curve.

AES has a flat shape over the wide range of the distance [11], the stability of this configuration becomes quite sensitive to the energy position of the threshold.

Let us consider the difference in the $J^\pi = 0^+$ and 1^- in relation to the inversion doublet structure. The $(\pi_{3/2}^-)^2$ AES in $J^\pi = 0^+$ and the $\alpha + {}^6\mathrm{He}_{g.s.}$ AES in $J^\pi = 1^-$ originally form the inversion doublet of $\alpha + {}^6\mathrm{He}_{g.s.}$ with $K^\pi = 0^\pm$. The $J^\pi = 0^+$ partner couples to the symmetric ${}^5\mathrm{He} + {}^5\mathrm{He}$ configuration and hence, it is strongly distorted to the molecular orbital as the distance S gets closer. In the $J^\pi = 1^-$ surface, however, the dinuclear configuration of $\alpha + {}^6\mathrm{He}_{g.s.}$ is well developed, which is similar situation to the ${}^{20}\mathrm{Ne} = \alpha + {}^{16}\mathrm{O}$ system [28]. Therefore, the appearance of the avoided crossing in the negative parity has a close connection to the formation of the inversion doublet in the compound system of ^{10}Be.

We next discuss how the AES profile and the level scheme appear in the low energy reactions. We show the partial cross section for the inelastic scattering to ${}^6\mathrm{He}(2_1^+)$ excitation. In solving the scattering problem, we employ the Kohn–Hulthén–Kato (KHK) variation method [29] where the AO basis in Eq. (1) are transformed to the asymptotic channel wave function. The present calculation is equivalent to the usual coupled-channels calculation including the channels of $\alpha + {}^6\mathrm{He}(0_1^+, 0_2^+, 2_1^+, 2_2^+, 1^+)$ and ${}^5\mathrm{He}(3/2^-, 1/2^-) + {}^5\mathrm{He}(3/2^-, 1/2^-)$. Our calculation thus includes much more channel components than the previous studies of $\alpha + {}^6$He cluster model [14]. In this calculation, the maximum S is changed from 70 fm to 12 fm and the channel wave function is matched to the scattering Coulomb wave function at a matching radius $R_C = 11.7$ fm.

The calculated partial inelastic cross sections are shown in the right part of Figs. 3 and 4. In $J^\pi = 0^+$, a strong peak appears at $E_{\mathrm{c.m.}} \sim 3$ MeV, although there is no definite avoided crossing in the AES. This is due to the effect of the radially-excited pole, 0_3^+, which include the large component of the exit 2_1^+ channel. We can also see the enhancements at $E_{\mathrm{c.m.}} \sim 7$ MeV, which nicely coincident to the adiabatic pole of $(\pi_{1/2}^-)^2$, 0_4^+, but it is much smaller than that generated by the radially-excited poles.

In $J^\pi = 1^-$, the strong enhancement can also be seen at $E_{\mathrm{c.m.}} \sim 6$ MeV, nevertheless there is no pole in the incident and exit channels. The energy of the enhancement is quite close to that of the avoided crossing at $S = 6$ fm. To investigate the origin of this enhancement, we have solved the coupled-channel problem between the lowest two AS by employing the adiabatic Kohn–Hulthén–Kato method that will be explained in the next paragraph. In such calculation, we have confirmed that this peak is generated by the coupling between the lowest two AS, nevertheless there appears no poles. Therefore, we can conclude that this inelastic peak is due to the LZ transition at the avoided crossing. Though the $(\pi_{1/2}^-\sigma_{1/2}^+)$ resonance is located close to the cross section peak, it weakly couples to the incident and exit channels. This pole is found to just generate the kink at a slightly lower energy than the peak position.

To see the connection between the AS and the scattering process in a transparent way, we formulate the adiabatic KHK (AKHK) method in which individual AS are employed as the basis functions in solving the scattering problem. In the following, we briefly explain the formulation of the AKHK. First, we define the ath AS at a distance S by

$$\Psi_{\mathrm{AS}}^{J^\pi a}(S) \equiv \sum_{iK} D_{iK}^a(S)\Phi_i^{J^\pi K}(S) = \sum_\beta F_\beta^a(S)\Phi_{\mathrm{CH}}^{J^\pi\beta}(S), \tag{3}$$

$$\Phi_{\mathrm{CH}}^{J^\pi\beta}(S) = \mathcal{A}\Big\{\Big[\big[\varphi_{1I_1}(\xi_1)\otimes\varphi_{2I_2}(\xi_2)\big]_I \otimes Y_L(\hat{\mathbf{R}})\Big]_{J^\pi} \times \chi_L(R,S)\Big\} \quad (\beta \equiv I_1 I_2 I L), \tag{4}$$

where $\Phi_i^{J^\pi K}(S)$ is the AO basis given by Eq. (1). In the second line, the AS is expanded in terms of the channel (CH) wave function, $\Phi_{\mathrm{CH}}^{J^\pi\beta}(S)$. Eq. (4) shows the explicit expression of $\Phi_{\mathrm{CH}}^{J^\pi\beta}(S)$ which is constructed from the angular momentum coupling among the internal states of ith nucleus $\varphi_{iI_iM_i}(\xi_i)$ and the spherical harmonics $Y_{LM}(\hat{\mathbf{R}})$ with the relative coordinate $\mathbf{R}$. In the last line of Eq. (4), $\chi_L(R,S)$ denotes the locally peaked Gaussian with the peak position of $R \sim S$.

The mixing coefficients in the ath AS, $F_\beta^a(S)$, satisfies the following relation

$$\lim_{S\to\infty} F_\beta^a(S) \sim \delta_{\beta,\alpha}. \tag{5}$$

Eq. (5) means that the ath AS becomes a specific channel α at an asymptotic region ($S \to \infty$), although a various channel components are strongly mixed in the internal region ($S \sim$ small). In solving the scattering problem with the basis of the AS, therefore, only a specific channel α satisfying Eq. (5) should be transformed into the scattering basis function, because the respective radial function $\chi_L(R,S)$ do not satisfy the scattering boundary condition.

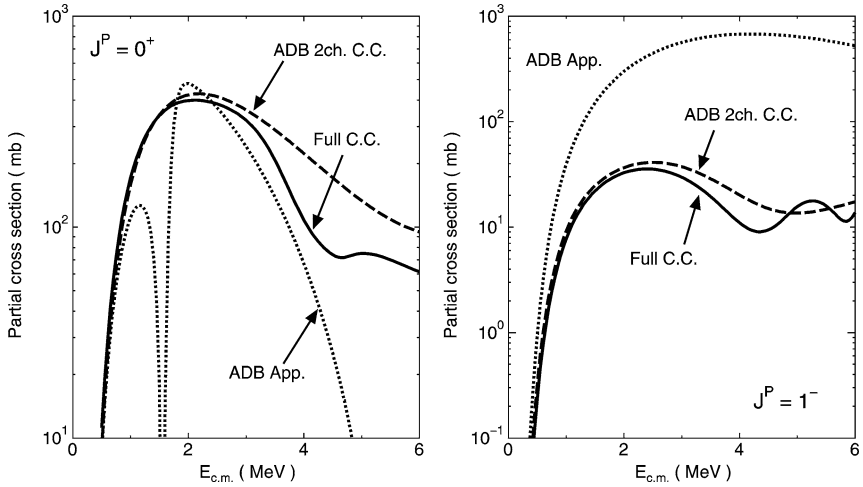

Fig. 5. The partial cross section of the $\alpha + {}^6\mathrm{He}_{\mathrm{g.s.}}$ elastic scattering. The left and right panels show the results for $J^\pi = 0^+$ and $J^\pi = 1^-$, respectively. The dotted curve shows the result of the adiabatic approximation, while the solid and dashed ones show that of two AS coupled-channel and that of the full coupled-channels, respectively.

The transformation can be done by utilizing the KHK method, in which the localized basis functions are smoothly connected to the scattering Coulomb wave function at a matching radius R_C [29]. The R_C should be taken to be sufficiently large value where all the channel components except for α are completely damped. The calculation of the matrix element for the AKHK basis can be easily done by the similar procedures shown in Ref. [29]. The details of the AKHK method will be shown in a forthcoming paper.

In order to discuss the gross features of the non-adiabatic effects, we calculate the partial cross sections of the elastic scattering. In two panels of Fig. 5, the results calculated from the AKHK method are shown. In this calculation, the $S_{\max}$ and the R_C are taken to be the same values in calculating the inelastic cross section. In both panels, the dotted curves show the pure adiabatic approximation. That is, only the AS along to the lowest AES is employed in solving the scattering problem. The solid curves show the solution of the full coupled channel (CC) in which all the AS are included.

In the result of $J^\pi = 0^+$, the adiabatic approximation quite nicely simulates the full CC solution in the low-energy region. Furthermore, the adiabatic approximation simulates the gross behavior of the full CC solution up to about 4 MeV except for the kink just below 2 MeV. This means that the elastic scattering mainly proceeds along to the lowest AES. The dashed curve shows the result in which the lowest two AS are coupled. The coupling effect improves the adiabatic approximation. The dashed curve deviates from the solid one in the higher energy than 3 MeV, but the difference is not so large.

The results of $J^\pi = 1^-$ is drastically different from those of $J^\pi = 0^+$. The validity of the adiabatic approximation is limited only in the region of the small cross section. Furthermore, the non-adiabatic coupling between the lowest two AS strongly reduces the cross section of the adiabatic approximation, which amounts to about one order reduction. Therefore, the adiabatic approximation is quite poor for describing the scattering process. The main contribution of the non-adiabatic coupling is from the first excited AS, because the dashed curve is similar to the solid one. This is due to the appearance of the avoided crossing which can be clearly seen in Fig. 2.

In summary, we investigated the adiabatic properties of the ${}^{10}\mathrm{Be} = \alpha + \alpha + N + N$ structures as well as the $\alpha + {}^6\mathrm{He}_{\mathrm{g.s.}}$ low-energy reactions, especially the non-adiabatic dynamics including the Landau–Zener (LZ) transition. We achieved such an unified study of the structures and the reactions in the generalized two-center cluster model (GTCM). The scattering problem in the GTCM is solved by applying the Kohn–Hulthén-Kato (KHK) variation method and the adiabatic KHK (AKHK) method proposed in the present study. We have found the non-adiabatic enhancements in the inelastic scattering cross-section to the $\alpha + {}^6\mathrm{He}(2_1^+)$ in both the $J^\pi = 0^+$ and $J^\pi = 1^-$ states. However, their origins are very different to each other. In the $J^\pi = 0^+$, the enhancements is due to the appearance of the radially-excited pole in the ${}^{10}\mathrm{Be}$ system. This is realized by the radial excitation of the α-core's relative motions. In contrast, the enhancement in $J^\pi = 1^-$ is originated from the LZ level-crossing between the lowest two adiabatic energy surfaces. Such a difference of the non-adiabatic dynamics also affects the elastic scattering process. In the positive parity, the adiabatic approximation is good for describing the collision process, while it becomes wrong approximation in the negative parity.

Next important step is to compare our result with recent experiments [6,7,9,10] by extending the present application to the higher partial waves. In a comparison with experiments, we should be careful to optimize the nucleon–nucleon interaction so as to reproduce the observed energy spectra in ${}^{10}\mathrm{Be}$ together with the threshold of $\alpha + {}^6\mathrm{He}$ and ${}^5\mathrm{He} + {}^5\mathrm{He}$. Such extended studies are under progress.

Acknowledgements

The author would like to thank Prof. K. Yabana for his valuable comments and careful check of the manuscript. He also

would like to thank to Prof. K. Kato and Prof. Y. Abe for their valuable discussions and encouragement. This work was performed as a part of the "Research Project for Study of Unstable Nuclei from Nuclear Cluster Aspects" at RIKEN.

References

[1] N. Itagaki, S. Okabe, Phys. Rev. C 61 (2000) 044306;
N. Itagaki, S. Okabe, K. Ikeda, Phys. Rev. C 62 (2000) 034301, and references therein.
[2] Y. Kanada-En'yo, H. Horiuchi, A. Dote, Phys. Rev. C 60 (1999) 064304;
Y. Kanada-En'yo, H. Horiuchi, A. Dote, Phys. Rev. C 66 (2002) 024305;
Y. Kanada-En'yo, H. Horiuchi, A. Dote, Phys. Rev. C 68 (2003) 014309.
[3] S. Ahmed, et al., Phys. Rev. C 69 (2004) 024303, and references therein.
[4] A. Saito, et al., Suppl. Prog. Theor. Phys. 146 (2003) 615.
[5] M. Milin, et al., Nucl. Phys. A 753 (2005) 263, and references therein.
[6] S. Shimoura, private communications.
[7] R. Raabe, et al., Phys. Rev. C 67 (2003) 044602.
[8] R. Raabe, et al., Nature 431 (2004) 823, and references therein.
[9] M. Freer, et al., Phys. Rev. Lett. 96 (2006) 042501.
[10] N. Soić, et al., private communications.
[11] M. Ito, K. Kato, K. Ikeda, Phys. Lett. B 588 (2004) 43;
M. Ito, K. Kato, K. Ikeda, in: Y. Suzuki, S. Ohya, M. Matsuo, T. Ohtsubo (Eds.), Proceedings of the International Symposium on a New Era of Nuclear Structure Physics, World Scientific, Singapore, 2004, p. 148.
[12] M. Ito, K. Yabana, K. Kato, K. Ikeda, J. Phys. Conference Ser. 20 (2005) 185.
[13] K. Arai, Phys. Rev. C 69 (2004) 014309.
[14] P. Descouvemont, D. Baye, Phys. Lett. B 505 (2001) 71;
D. Baye, P. Descouvemont, R. Kamouni, Few-Body Systems 29 (2000) 131.
[15] K. Fujimura, D. Baye, P. Descouvemont, Y. Suzuki, K. Varga, Phys. Rev. C 59 (1999) 817;
P. Descouvemont, Nucl. Phys. A 699 (2002) 463.
[16] Y. Ogawa, K. Arai, Y. Suzuki, K. Varga, Nucl. Phys. A 673 (2000) 122.
[17] Y. Abe, J.Y. Park, Phys. Rev. C 28 (1983) 2316.
[18] N. Cindro, R.M. Freeman, F. Haas, Phys. Rev. C 33 (1986) 1280.
[19] J.Y. Park, K. Gramlich, W. Scheid, W. Greiner, Phys. Rev. C 33 (1986) 1674.
[20] M.H. Cha, J.Y. Park, W. Scheid, Phys. Rev. C 36 (1987) 2341.
[21] T. Tazawa, Y. Abe, Phys. Rev. C 41 (1990) R17;
T. Tazawa, Y. Abe, Prog. Theor. Phys. 85 (1991) 567.
[22] B. Imanishi, W. von Oertzen, H. Voit, Phys. Rev. C 35 (1987) 359;
B. Imanishi, W. von Oertzen, Phys. Rep. 155 (1987) 29.
[23] See, for example, L.D. Landau, E.M. Lifshitz, Quantum Mechanics, third ed., Elsevier, Butterworth–Heinemann, 1958;
H. Nakamura, Nonadiabatic Transition, World Scientific, Singapore, 2000, and references therein.
[24] R.M. Freeman, C. Beck, H. Haas, B. Ueusch, J.J. Kolata, Phys. Rev. C 28 (1983) 437;
C. Beck, R.M. Freeman, H. Haas, B. Ueusch, J.J. Kolata, Nucl. Phys. A 443 (1985) 157.
[25] R.M. Freeman, Z. Basrak, F. Hass, A. Hachem, G.A. Monehan, A. Morsad, M. Youlal, Phys. Rev. C 38 (1988) 1081.
[26] H. Horiuchi, et al., Suppl. Prog. Theor. Phys. 62 (1977) 1, and references therein.
[27] M. Ito, K. Yabana, Prog. Theor. Phys. 113 (2005) 1047.
[28] H. Horiuchi, et al., Suppl. Prog. Theor. Phys. 52 (1972) 1;
H. Horiuchi, et al., Suppl. Prog. Theor. Phys. 68 (1980) 1, and references therein.
[29] M. Kamimura, Prog. Theor. Phys. Suppl. 62 (1977) 236.